Letters

Comparative Study of the Active and Passive Circulating Current Suppression Methods for Modular Multilevel Converters

Binbin Li, *Member, IEEE*, Zigao Xu, Shaolei Shi, Dianguo Xu, *Fellow, IEEE*, and Wei Wang

***Abstract*—Circulating current is an undesirable phenomenon in modular multilevel converter which should be attenuated to reduce current stress and power losses. This letter presents a comparative study of the active and passive circulating current suppression methods. Voltage penalty of the active circulating current control is derived, and design of the passive circulating current filter parameters is provided. Simulations and experiments are performed to validate the analysis.**

***Index Terms*—Circulating current, modular multilevel converter (MMC), passive filter, voltage penalty.**

I. Introduction

MODULAR multilevel converters (MMCs) have emerged as one of the most competitive voltage source converter (VSC) topologies for high-voltage and large-power applications, and have already given rise to an upsurge in the use of VSC-HVDC for integration of wind farms as well as interconnection of grids between countries [1], [2]. However, one unique characteristic of MMC is the existence of circulating current [3]. If not suppressed, the circulating current would distort the arm currents, increase power losses, and cause higher current stresses on the semiconductor devices.

The circulating current can be eliminated by active control of the MMC arm voltages and various control methods have been proposed. Since stationary PI control has limited gain for ac signals, a double-line-frequency rotational-frame PI controller was employed in [4] which can effectively suppress the most predominant harmonic component (i.e., second-order) in the circulating current. But the drawback of this method is the inability to cope with unbalanced three-phase conditions. To solve this problem, a series of paralleled proportional resonant controllers have been proposed in [5] and [6] which show good circulating current suppression performance at the selected resonant frequency and do not need to consider three-phase unbalances. Besides, the repetitive controller can also be adopted, which in theory is equivalent to a series of resonant controllers [7], [8]. In [9], the circulating current control was further integrated into modulation stage by utilizing redundant voltage states of MMC, operating like a hysteresis control. This approach features the advantages of simple implementation and quick dynamic response. Alternatively, the circulating current can also be attenuated by using passive filters. Tu *et al*. [10] analyzed the influence of arm inductance on the amplitude of the circulating currents. Increasing the arm inductance can result in a smaller circulating current, but the inductance would become excessively large if satisfactory suppression is required, which is very costly and cumbersome. In [11], a parallel resonant circuit was developed through a tap of the MMC arm inductors in parallel with a capacitor; thus, the second-order circulating current can be completely eliminated without increasing the arm inductance.

Compared with the passive circulating current suppression methods, active control seems to be superior as it does not bring additional hardware cost. But practically, in order to suppress circulating current, the active control consumes a certain amount of MMC voltage which means the maximum available output voltage as well as the power capacity of MMC has to be curtailed. In this letter, penalties of the output voltage and power capacity with respect to the active circulating current suppression are analyzed. Moreover, the design of the passive circulating current filter parameters is also presented. The results can be used to weigh the voltage penalty of active control against the additional hardware cost of passive filters. Finally, simulations and experimental results prove the validity of the analysis and parameter design.

II. Voltage Penalty Analysis of the Active Circulating Current Suppression Method

The circuit configuration of MMC is shown in Fig. 1. Each phase of it consists of two arms, the upper and the lower, which are connected through two buffer inductors L_0 and parasitic resistors R_0. Each arm is formed by a total of N identical submodule (SMs), and each SM contains a dc storage capacitor $C_{\rm SM}$ and two insulated gate bipolar transistor (IGBTs) (i.e., S_1 and S_2). With appropriate voltage balancing control, the average voltage of each SM capacitor is equal to $U_{\rm dc}/N$. $U_{\rm dc}$ is the dc-link voltage, and u_o and i_o are the output ac voltage and current,

Manuscript received May 21, 2017; revised July 4, 2017; accepted August 5, 2017. Date of publication August 8, 2017; date of current version December 1, 2017. *(Corresponding author: Binbin Li.)*

The authors are with the School of Electrical Engineering and Automation, Harbin Institute of Technology, Harbin 150001, China (e-mail: libinbin@hit.edu.cn; jz13503581249@163.com; 373841185@qq.com; xudiang@hit.edu.cn; wangwei602@hit.edu.cn).

Color versions of one or more of the figures in this letter are available online at http://ieeexplore.ieee.org.

Digital Object Identifier 10.1109/TPEL.2017.2737541

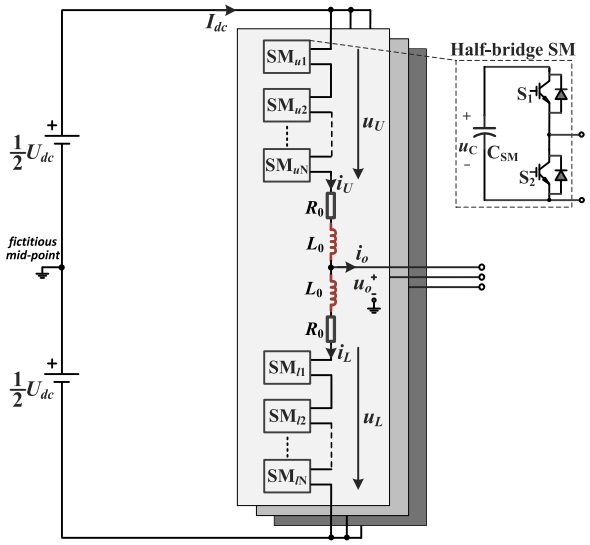

Fig. 1. Circuit configuration of MMC.

respectively. u_U and i_U are the voltage and current of the upper arm, and u_L and i_L are the voltage and current of the lower arm, respectively. The following equations can be obtained according to Kirchhoff's voltage law:

$$u_L + u_U = U_{\rm dc} - 2R_0 i_c - 2L_0 \frac{di_c}{dt} \tag{1a}$$

$$u_e = \tfrac{1}{2}\left(u_L - u_U\right) = u_o + \tfrac{1}{2}R_0 i_o + \tfrac{1}{2}L_0 \frac{di_o}{dt} \tag{1b}$$

where i_c is the circulating current given by $i_c = \frac{1}{2}(i_U + i_L)$. u_e is denoted as MMC inner ac voltage [12], which is expressed as

$$u_e = U_e \cos\left(\omega t\right) \tag{2}$$

where U_e is the voltage amplitude.

Thus, MMC ac output voltage and current can be expressed as

$$u_o = U_o \cos\left(\omega t - \theta\right) \tag{3a}$$

$$i_o = I_o \cos\left(\omega t - \varphi\right) \tag{3b}$$

where U_o and I_o are the amplitudes, ω is the angular frequency, and θ and φ are the phase lag angles. Note that u_o and u_e are slightly different as they represent the voltages before and after the arm reactance, respectively.

Ideally, MMC arm voltage references are given as

$$u_{{\rm ref}\_U} = \tfrac{1}{2}\left(1 - m_1 \cos(\omega t + \delta_1)\right) \tag{4a}$$

$$u_{{\rm ref}\_L} = \tfrac{1}{2}\left(1 + m_1 \cos(\omega t + \delta_1)\right) \tag{4b}$$

where m_1 and δ_1 are the modulation index and phase angle of the fundamental component, respectively.

However, if active control methods are applied to eliminate the second-order circulating current harmonics, a second-order component would be generated in the arm voltage references, and thereby (4) is modified as

$$u_{{\rm ref}\_U} = \tfrac{1}{2}\left(1 - m_1 \cos(\omega t + \delta_1) + m_2 \cos(2\omega t + \delta_2)\right) \tag{5a}$$

$$u_{{\rm ref}\_L} = \tfrac{1}{2}\left(1 + m_1 \cos(\omega t + \delta_1) + m_2 \cos(2\omega t + \delta_2)\right) \tag{5b}$$

where m_2 and δ_2 are the modulation index and phase angle of the second-order component, respectively.

Since the circulating current is eliminated, the upper and lower arm currents of MMC can be expressed as

$$i_U = \tfrac{1}{3}I_{\rm dc} + \tfrac{1}{2}I_o \cos\left(\omega t - \varphi\right) \tag{6a}$$

$$i_L = \tfrac{1}{3}I_{\rm dc} - \tfrac{1}{2}I_o \cos\left(\omega t - \varphi\right) \tag{6b}$$

where $I_{\rm dc}$ is the dc-link current.

The capacitor voltage of the upper and lower arm SMs can thus be obtained as

$$u_{C\_U} = \frac{1}{C_{\rm SM}} \int i_U\, u_{{\rm ref}\_U}\, dt + \frac{U_{\rm dc}}{N} \tag{7a}$$

$$u_{C\_L} = \frac{1}{C_{\rm SM}} \int i_L\, u_{{\rm ref}\_L}\, dt + \frac{U_{\rm dc}}{N}. \tag{7b}$$

According to the power balance of MMC between dc input and ac output (i.e., $U_{\rm dc}I_{\rm dc} = \frac{3}{2}\, U_o I_o \cos\varphi$), we have $I_{\rm dc} = \frac{3}{4} I_o m_1 \cos\varphi$. Substituting (5) and (6) into (7) leads to

$$\begin{aligned} u_{C\_U} = {} & \frac{U_{\rm dc}}{N} + \frac{1}{48\omega C_{\rm SM}} \left[-8I_{\rm dc} m_1 \sin\left(\omega t + \delta_1\right)\right. \\ & + 12 I_o \sin\left(\omega t - \varphi\right) + 6 I_o m_2 \sin\left(\omega t + \varphi + \delta_2\right) \\ & - 3 I_o m_1 \sin\left(2\omega t + \delta_1 - \varphi\right) + 4 I_{\rm dc} m_2 \sin\left(2\omega t + \delta_2\right) \\ & \left. + 2 I_o m_2 \sin\left(3\omega t - \varphi + \delta_2\right)\right] \end{aligned} \tag{8a}$$

$$\begin{aligned} u_{C\_L} = {} & \frac{U_{\rm dc}}{N} + \frac{1}{48\omega C_{\rm SM}} \left[8I_{\rm dc} m_1 \sin\left(\omega t + \delta_1\right)\right. \\ & - 12 I_o \sin\left(\omega t - \varphi\right) - 6 I_o m_2 \sin\left(\omega t + \varphi + \delta_2\right) \\ & - 3 I_o m_1 \sin\left(2\omega t + \delta_1 - \varphi\right) + 4 I_{\rm dc} m_2 \sin\left(2\omega t + \delta_2\right) \\ & \left. - 2 I_o m_2 \sin\left(3\omega t - \varphi + \delta_2\right)\right]. \end{aligned} \tag{8b}$$

According to (5) and (8), MMC arm voltages can be derived as

$$u_U = N u_{{\rm ref}\_U} u_{C\_U} \approx -u_1 + u_2 + \tfrac{3}{2}U_{\rm dc} \tag{9a}$$

$$u_L = N u_{{\rm ref}\_L} u_{C\_L} \approx u_1 + u_2 + \tfrac{1}{2}U_{\rm dc} \tag{9b}$$

where u_1 and u_2 are the fundamental and second-order voltage components, respectively, as

$$\begin{aligned} u_1 = {} & \frac{1}{2} m_1 U_{\rm dc} \cos\left(\omega t + \delta_1\right) + \frac{N}{192\omega C_{\rm SM}} \\ & \times \left[-24 I_o \sin\left(\omega t - \varphi\right) + \left(4m_2^2 - 3m_1^2\right) I_o \sin\left(\omega t - \varphi\right)\right. \\ & \left. - 4 I_{\rm dc} m_1 m_2 \sin\left(\omega t - \delta_1 + \delta_2\right) + 16 I_{\rm dc} m_1 \sin\left(\omega t + \delta_1\right)\right] \end{aligned} \tag{10}$$

$$u_2 = \frac{1}{2}m_2 U_{\rm dc}\cos(2\omega t+\delta_2) + \frac{N}{96\omega C_{\rm SM}} \times \left[-9I_o m_1 \sin(2\omega t+\delta_1-\varphi) + 4I_{\rm dc} m_2 \sin(2\omega t+\delta_2) - I_o m_1 m_2 \sin(2\omega t-\delta_1+\delta_2-\varphi) - 3I_o m_1 m_2 \sin(2\omega t+\delta_1+\delta_2+\varphi) + 4I_{\rm dc} m_1^2 \sin(2\omega t+2\delta_1)\right]. \quad (11)$$

Note that the "≈" sign is used in (9) because there are also third-, fourth-, and fifth-order voltage components. But these components are relatively small and their frequencies are not relevant to the circulating current analysis. Therefore, they are neglected here for simplicity.

Equations (10) and (11) can be further decomposed into sine and cosine components, that is, $u_1 = U_{1\_\sin}\sin(\omega t) + U_{1\_\cos}\cos(\omega t)$ and $u_2 = U_{2\_\sin}\sin(2\omega t) + U_{2\_\cos}\cos(2\omega t)$, with

$$U_{1\_\sin} = -\frac{1}{2}m_1 U_{\rm dc}\sin(\delta_1) + \frac{N}{192\omega C_{\rm SM}} \times \left[-4I_{\rm dc} m_1 m_2 \cos(\delta_2-\delta_1) + 16 I_{\rm dc} m_1 \cos(\delta_1) - \left(24+3m_1^2-4m_2^2\right) I_o \cos(\varphi)\right] \quad (12a)$$

$$U_{1\_\cos} = \frac{1}{2}m_1 U_{\rm dc}\cos(\delta_1) + \frac{N}{192\omega C_{\rm SM}} \times \left[-4I_{\rm dc} m_1 m_2 \sin(\delta_2-\delta_1) + 16 I_{\rm dc} m_1 \sin(\delta_1) + \left(24+3m_1^2-4m_2^2\right) I_o \sin(\varphi)\right] \quad (12b)$$

$$U_{2\_\sin} = -\frac{1}{2}m_2 U_{\rm dc}\sin(\delta_2) + \frac{N}{96\omega C_{\rm SM}} \times \left[4I_{\rm dc} m_1^2 \cos(2\delta_1) - 9I_o m_1 \cos(\delta_1-\varphi) + 4I_{\rm dc} m_2 \cos(\delta_2) - 3I_o m_1 m_2 \cos(\delta_2+\varphi+\delta_1) - I_o m_1 m_2 \cos(\delta_2-\varphi-\delta_1)\right] \quad (13a)$$

$$U_{2\_\cos} = \frac{1}{2}m_2 U_{\rm dc} cos(\delta_2) + \frac{N}{96\omega C_{\rm SM}} \times \left[4I_{\rm dc} m_1^2 \sin(2\delta_1) - 9I_o m_1 \sin(\delta_1-\varphi) + 4I_{\rm dc} m_2 \sin(\delta_2) - 3I_o m_1 m_2 \sin(\delta_2+\varphi+\delta_1) - I_o m_1 m_2 \sin(\delta_2-\varphi-\delta_1)\right]. \quad (13b)$$

Subtracting (9a) and (9b), it is found that u_1 is actually the inner ac voltage of MMC, which needs to comply with (1b), giving

$$U_{1\_\cos} = U_e \quad \text{and} \quad U_{1\_\sin} = 0. \quad (14)$$

On the other hand, since the second-order circulating current is controlled to zero. According to (1a), sum of (9a) and (9b) should be zero, which gives

$$U_{2\_\cos} = 0 \quad \text{and} \quad U_{2\_\sin} = 0. \quad (15)$$

Equations (14) and (15) are a system of four nonlinear equations with unknown variables of m_1, δ_1, m_2, and δ_2, these variables can be solved by numerical iterative methods (such as the built-in *"fsolve"* function in the MATLAB software). As a result, the modulation index penalty of MMC with active circulating current control can be calculated by

$$\Delta m = \max\left(\left|m_1\cos(\omega t+\delta_1) + m_2\cos(2\omega t+\delta_2)\right|\right) - m_1. \quad (16)$$

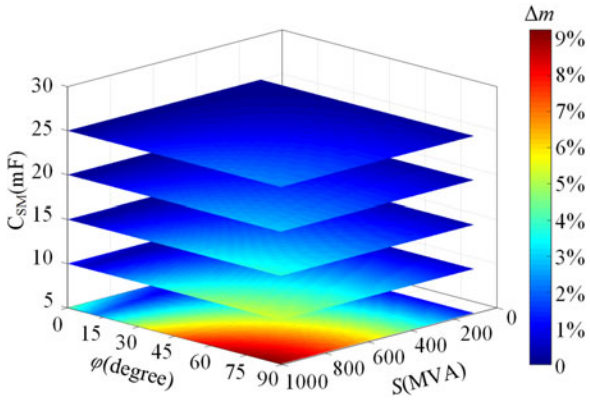

Fig. 2. MMC modulation index penalty of active circulating current suppression, with respect to SM capacitance CSM, phase lag angle φ, and apparent power S.

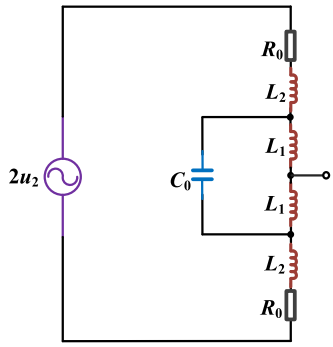

Fig. 3. Circuit structure of hardware circulating current filters.

Fig. 2 analyzes the modulation index penalty with respect to different SM capacitance $C_{\rm SM}$, power factor angle φ, and apparent power S, at the conditions of $U_{\rm dc}/N = 2\text{kV}, m = 0.8$, and $\omega = 100\pi$ rad/ s, respectively. It is shown that Δm increases with S and decreases with $C_{\rm SM}$, and the maximum Δm can exceed 9%. The voltage penalty can be easily obtained as $\frac{1}{2}\Delta m U_{\rm dc}$, which means the maximum available MMC ac voltage is reduced. The power capacity penalty of MMC is then $\Delta m S$. This implies $\Delta m S$ MMC installed capacity has been wasted. Therefore, when applying the active circulating current suppression method, the voltage and power penalties must be taken into consideration.

III. Parameter Dimensioning of the Passive Circulating Current Filter

Circuit structure of the passive circulating current filter is depicted in Fig. 3. The original MMC arm inductor is split into to two (L_1, L_2), of which L_1 and C_0 are used to form a parallel-resonant filter and L_2 is utilized to ensure the total arm inductance unchanged, i.e., $L_1 + L_2 = L_0$.

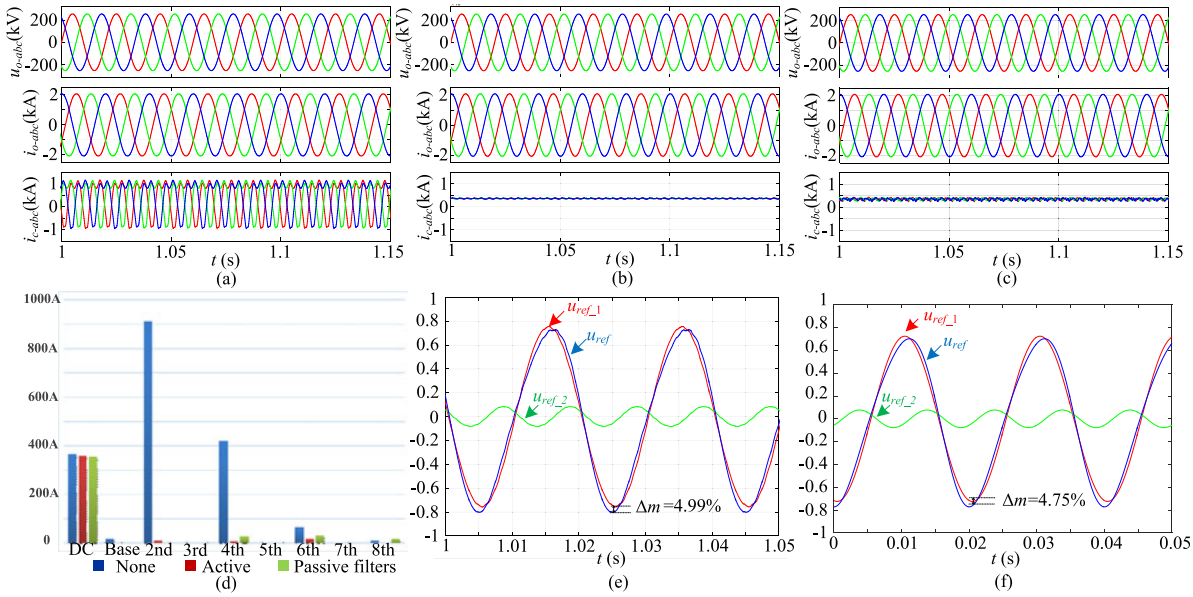

Fig. 4. Simulation results of MMC with different circulating current suppression methods, (a) without suppression, (b) active suppression, (c) passive suppression, (d) FFT harmonic spectrums, (e) simulated reference waveforms with active suppression, and (f) analytically calculated reference waveforms with active suppression.

TABLE I
MMC SIMULATION PARAMETERS

Quantity	Value
Number of SMs per arm	$N = 320$
DC-link voltage	$U_{\text{dc}} = 640$ kV
Average SM capacitor voltage	$U_{C\,(\text{rated})} = 2000$ V
SM capacitance	$C_{\text{SM}} = 5000\ \mu$F
Apparent power	$S = 806$ MVA
Power factor	$\cos\varphi = 0.844$
Fundamental angular frequency	$\omega = 100\pi$ rad/ s
Total arm inductance	$L_0 = 10$ mH
Arm inductance 1	$L_1 = 5.56$ mH
Arm inductance 2	$L_2 = 4.44$ mH
Filter capacitance	$C_0 = 227.79\ \mu$F

TABLE II
THEORETICAL AND SIMULATED MODULATION INDEX PENALTY

Quantity	Theoretical value	Simulated value
Peak value of $u_{\text{ref\_1}}$	$m_1 = 0.7246$	$m_1 = 0.753$
Phase angle of $u_{\text{ref\_1}}$	$\delta_1 = -8.54°$	$\delta_1 = -8.11°$
Peak value of $u_{\text{ref\_2}}$	$m_2 = 0.0773$	$m_2 = 0.0824$
Phase angle of $u_{\text{ref\_2}}$	$\delta_2 = 135.96°$	$\delta_2 = 136.40°$
Modulation index penalty	$\Delta m = 4.75\%$	$\Delta m = 4.99\%$

The filter impedance can be expressed as

$$Z(j\omega) = 2R_0 + j\frac{4\omega^3 L_1 L_2 C_0 - 2\omega(L_1 + L_2)}{2\omega^2 L_1 C_0 - 1} \tag{17}$$

where a parallel resonance and a series resonance can be derived, respectively, as

$$\omega_p = \sqrt{\frac{1}{2L_1 C_0}} \tag{18}$$

$$\omega_s = \sqrt{\frac{L_1 + L_2}{2L_1 L_2 C_0}}. \tag{19}$$

Fig. 5. Photograph of the laboratorial three-phase MMC prototype.

To suppress the second-order circulating current harmonic, ω_p needs to be selected at 2ω. Meanwhile, the series resonant frequency ω_s can be selected at odd-order frequency to avoid amplifying any other even-order circulating current harmonics. As such, parameters of the passive circulating current filter can be designed as

$$L_2 = \left(\frac{2\omega}{\omega_s}\right)^2 L_0 \tag{20}$$

$$L_1 = L_0 - L_2 \tag{21}$$

$$C_0 = \frac{1}{2L_1(2\omega)^2}. \tag{22}$$

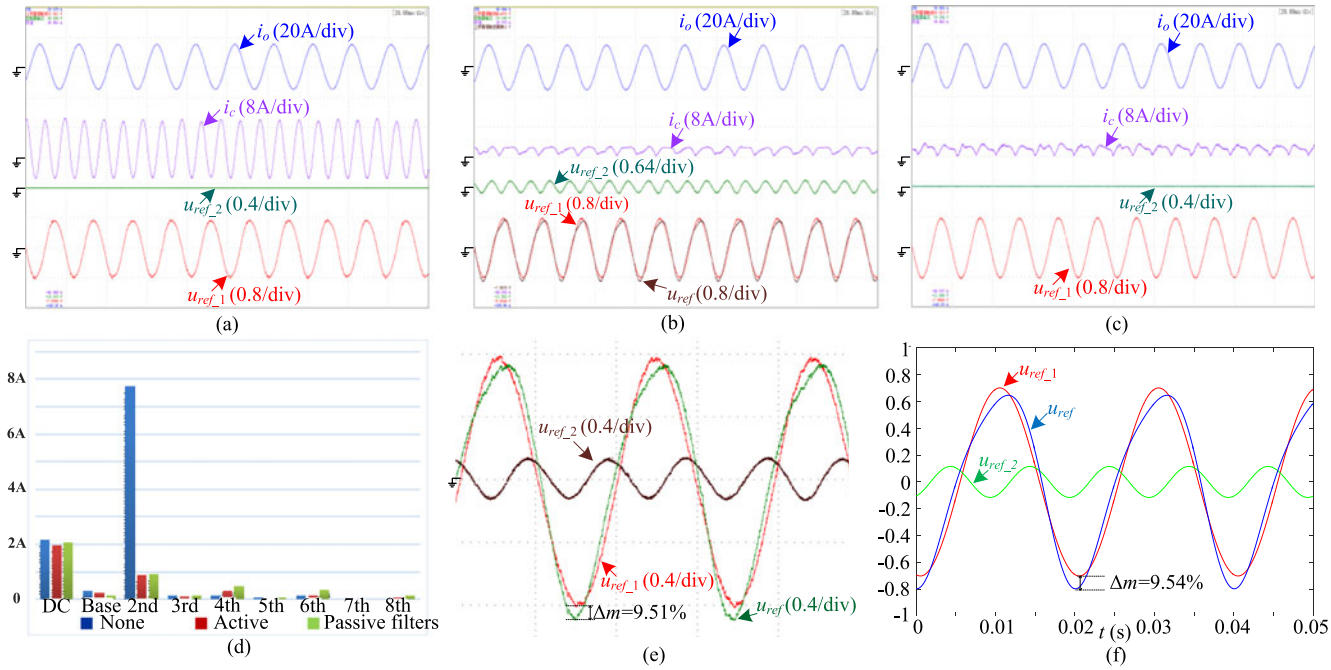

Fig. 6. Experimental results with different circulating current suppression methods, (a) without suppression, (b) active suppression, (c) passive suppression, (d) FFT harmonic spectrums, (e) experimental reference waveforms with active suppression, and (f) analytically calculated reference waveforms with active suppression.

Since the passive filter does not increase the total arm inductance, the extra hardware cost of MMC is mainly the resonant capacitor C_0. Besides the capacitance value of (22), its voltage and current ratings should also be determined.

When passive filters are employed, the MMC arm voltage references become (4), not containing second-order component. Thus, by substituting $m_2 = 0$ and $\delta_2 = 0$ into (11), u_2 becomes

$$u_2 = \frac{N}{96\omega C_{\rm SM}} \left[-9I_o m_1 \sin\left(2\omega t + \delta_1 - \varphi\right) + 4I_{\rm dc} m_1^2 \sin\left(2\omega t + 2\delta_1\right)\right]. \tag{25}$$

The second-order voltages of both the upper and lower arms are blocked by the parallel resonant circuit. Voltage rating of the resonant capacitor must be higher than twice the amplitude of u_2, which is, (24) shown at the bottom of this page, and current rating of the resonant capacitor is thus $2\omega C_0 U_{C0}$.

Therefore, given an MMC circuit, the extra hardware cost of the passive method can be weighed against the power capacity penalty of the active counterpart, so as to determine the most cost-effective circulating current suppression solution.

IV. Simulation and Experimental Results

A. Simulation Verification

To verify the effectiveness of the modulation index penalty analysis and the parameter design of the passive filter, a three-phase MMC inverter was simulated based on MATLAB/Simulink. The simulation parameters are listed in Table I. The simulation waveforms of MMC without circulating current suppression, with active suppression, and with passive suppression are shown in Fig. 4(a), (b), and (c), respectively. Performing fast Fourier transform (FFT) transformation to these circulating current waveforms, the detailed harmonic features are obtained in Fig. 4(d). It can be seen that without suppression, there were significant harmonics in the circulating current with the second-order harmonic amplitude up to 900 A. When either the active or the passive suppression was applied, the circulating current harmonics were almost eliminated, confirming the same effectiveness of both methods.

Fig. 4(e) shows the simulated MMC voltage references, including the fundamental component $u_{\rm ref\_1}$, the second-order component $u_{\rm ref\_2}$, and the synthesized reference $u_{\rm ref}$. It is clear that with active suppression, peak value of $u_{\rm ref}$ was higher than that of $u_{\rm ref\_1}$ in MMC without circulating current suppression or with passive suppression, revealing the modulation index penalty of $\Delta m = 4.99\%$. Fig. 4(f) shows the analytically calculated voltage references. Then, the detailed waveform parameters of Fig. 4(e) and (f) are extracted and compared in Table II. The analyzed and simulated values are found to be in good agreement.

B. Experimental Verification

A scaled down laboratory three-phase MMC prototype with seven half-bridge SMs per arm, as shown in Fig. 5, has been built and tested. The circuit parameters and operating conditions are listed in Table III. The experimental waveforms without

$$U_{C_0} \geq \frac{N}{48\omega C_{\rm SM}} \sqrt{\left(4I_{\rm dc}m_1^2 \sin\left(2\delta_1\right) - 9I_o m_1 \sin\left(\delta_1 - \varphi\right)\right)^2 + \left(4I_{\rm dc}m_1^2 \cos\left(2\delta_1\right) - 9I_o m_1 \cos\left(\delta_1 - \varphi\right)\right)^2} \tag{24}$$

TABLE III
EXPERIMENTAL PARAMETERS

Quantity	Value
Number of SMs per arm	$N = 7$
DC-link voltage	$U_{\text{dc}} = 350$ V
Average SM capacitor voltage	$U_{C\,(\text{rated})} = 50$ V
SM capacitance	$C_{\text{SM}} = 1000\,\mu$F
Apparent power	$S = 3430$ VA
Power factor	$\cos\varphi = 0.640$
Fundamental angular frequency	$\omega = 100\pi$ rad/ s
Total arm inductance	$L_0 = 8$ mH
Arm inductance 1	$L_1 = 4$ mH
Arm inductance 2	$L_2 = 4$ mH
Filter capacitance	$C_0 = 300\,\mu$F

TABLE IV
THEORETICAL AND EXPERIMENTAL MODULATION INDEX PENALTY

Quantity	Theoretical value	Experimental value
Peak value of $u_{\text{ref\_1}}$	$m_1 = 0.7011$	$m_1 = 0.798$
Phase angle of $u_{\text{ref\_1}}$	$\delta_1 = -9.58^\circ$	$\delta_1 = -6.92^\circ$
Peak value of $u_{\text{ref\_2}}$	$m_2 = 0.1156$	$m_2 = 0.128$
Phase angle of $u_{\text{ref\_2}}$	$\delta_2 = 155.44^\circ$	$\delta_2 = 158.1^\circ$
Modulation index penalty	$\Delta m = 9.54\%$	$\Delta m = 9.51\%$

circulating current suppression, with active suppression, and with passive suppression are shown in Fig. 6(a), (b), and (c), respectively. According to the harmonic features of different methods, as indicated in Fig. 6(d), it can be found that circulating current suppression performances of the active and passive methods are almost the same.

From Fig. 6(e), the modulation index penalty of the MMC prototype can be observed as $\Delta m = 9.51\%$, which agrees well with the analytical value shown in Fig. 6(f). This can also be confirmed by comparison of the detailed waveform parameters presented in Table IV. Note that the experimental m_1 is larger than its theoretical value. This is mainly due to the voltage drop of the IGBTs. As voltage rating of the SMs in this experiment is only 50 V, the IGBT voltage drop becomes quite significant, and m_1 has to be larger to compensate this voltage drop.

V. CONCLUSION

The existence of circulating current is a unique characteristic of MMC, which should be suppressed to avoid causing higher losses or current stresses. The main contribution of this letter is providing a comparative study of the active and passive circulating current suppression methods. Voltage and power capacity penalties of the active control are derived, and design of the passive filter parameters is presented. These results can be weighed to determine the most cost-effective circulating current suppression method for an MMC. Finally, validity and effectiveness of the analysis have been confirmed by simulations and experimental results.

REFERENCES

[1] A. Lesnicar and R. Marquardt, "An innovative modular multilevel converter topology suitable for a wide power range," in *Proc. IEEE Power Tech. Conf.*, vol. 3, Bologna, Italy, Jun. 2003, p. 6.

[2] M. A. Perez, S. Bernet, J. Rodriguez, S. Kouro, and R. Lizana, "Circuit topologies, modeling, control schemes, and applications of modular multilevel converters," *IEEE Trans. Power Electron.*, vol. 30, no. 1, pp. 4–14, Jan. 2015.

[3] K. Ilves, A. Antonopoulos, S. Norrga, and H.-P. Nee, "Steady-state analysis of interaction between harmonic components of arm and line quantities of modular multilevel converters," *IEEE Trans. Power Electron.*, vol. 27, no. 1, pp. 57–68, Jan. 2012.

[4] Q. Tu, Z. Xu, and L. Xu, "Reduced switching-frequency modulation and circulating current suppression for modular multilevel PWM Converters," *IEEE Trans. Power Del.*, vol. 26, no. 3, pp. 2009–2017, Jul. 2011.

[5] Z. Li, P. Wang, Z. Chu, H. Zhu, Y. Luo, and Y. Li, "An inner current suppressing method for modular multilevel converters," *IEEE Trans. Power Electron.*, vol. 28, no. 11, pp. 4873–4879, Nov. 2013.

[6] S. Li, X. Wang, Z. Yao, T. Li, and Z. Peng, "Circulating current suppressing strategy for MMC-HVDC based on nonideal proportional resonant controllers under unbalanced grid conditions," *IEEE Trans. Power Electron.*, vol. 30, no. 1, pp. 387–397, Jan. 2015.

[7] M. Zhang, L. Huang, W. Yao, and Z. Lu, "Circulating harmonic current elimination of a CPS-PWM-based modular multilevel converter with a plug-in repetitive controller," *IEEE Trans. Power Electron.*, vol. 29, no. 4, pp. 2083–2097, Apr. 2014.

[8] B. Li, D. Xu, and D. Xu, "Circulating current harmonics suppression of modular multilevel converter based on repetitive control," *J. Power Electron.*, vol. 14, no. 6, pp. 1100–1108, Nov. 2014.

[9] G. Konstantinou, J. Pou, S. Ceballos, R. Picas, J. Zaragoza, and V. G. Agelidis, "Control of circulating currents in modular multilevel converters through redundant voltage levels," *IEEE Trans. Power Electron.*, vol. 31, no. 11, pp. 7761–7769, Nov. 2016.

[10] Q. Tu, Z. Xu, H. Huang, and J. Zhang, "Parameter design principle of the arm inductor in modular multilevel converter based HVDC," in *Proc. Int. Conf. Power Syst. Technol.*, 2010, pp. 1–6.

[11] B. Jacobson, P. Karlsson, G. Asplund, L. Harbefors, and T. Jonsson, "VSC-HVDC transmission with cascaded two-level converters," in *Proc. CIGRE2010*, Paris, France, 2010, pp. B4–B110.

[12] A. Antonopoulos, L. Angquist, and H.-P. Nee, "On dynamics and voltage control of the modular multilevel converter," in *Proc. Eur. Conf. Power Electron. Appl.*, 2009, pp. 1–10.